≪Review Paper≫ Applied Science and Convergence Technology Vol.23 No.1, January 2014, pp.1~13
http://dx.doi.org/10.5757/ASCT.2014.23.1.1

Magneto-optical Measurements of Semiconductor Quantum Structures in Pulsed-magnetic Fields

Yongmin Kim*

Department of Applied Physics and Institute of Nanosensor and Biotechnology, Dankook University, Yongin 448-701

(Received January 19, 2014, Revised January 30, 2014, Accepted January 30, 2014)

Semiconductor quantum structures are often characterized by their energy gaps which are modified by the quantum size effect. Energy levels in semiconductors can be realized by optical transitions within confined structures. Photoluminescence spectroscopy in magnetic fields at low temperatures has proved to be a powerful technique for investigating the electronic states of quantum semiconductor heterostructures and offers a complimentary tool to electrical transport studies. In this review, we examine comprehensive investigations of magneto-excitonic and Landau transitions in a large variety of undoped and doped quantum-well structures. Strong magnetic fields change the diamagnetic energy shift of free excitons from quadratic to linear in B in undoped single quantum well samples. Two-dimensional electron gas induced by modulation doping shows pronounce quantum oscillations in integer quantum Hall regime and discontinuous transition at ν=1. Such discontinuous transition can be explained as the formation of spin waves or Skyrmions.

Keywords : Photoluminescence, Magnetic field, Quantum well, Spin wave, Skyrmion

I. Introduction

A simplest quantum confined structure of semiconductors can be achieved by attaching two different semiconductors with different energy band gap. Deposition of two different semiconductor layers (typically <100 Å) repeatedly, a completely new type of two-dimensional (2D) carrier properties can be established. Such low dimensionality exhibits noble properties such as integer [1] and fractional [2] quantum Hall effects, quantum confined stark effect, and so on. Optical spectroscopy at low temperature (typically below 4 K) and high magnetic fields has proved to be a powerful tool for investigating the ground and excited states of high-quality quantum-well-type 2D semiconductor heterostructures [3] because optical transitions are strongly influenced by electron-electron interactions and the experimental method offers a complimentary tool to electrical transport studies.

1. Generation of pulsed-magnetic fields

Continuous magnetic fields can be achieved up to 45 tesla (T) by using a hybrid magnet which is concentrically consisted by an outer superconducting and inner resistive magnets. In comparison, the average magnetic field of the earth is about 5×10^{-5} T.

* [E-mail] yongmin@dankook.ac.kr

Because a superconducting magnet consumes large amount of liquid helium (L^4He) while a resistive magnet requires huge amount of electric power, a hybrid magnet, which has high developing and maintenance costs, becomes inefficient system to generate high magnetic fields. Therefore, a different type of high-field magnet with low developing and maintenance costs is required. To generate more than 50 T, pulsed magnet systems are widely used. Normally, capacitor bank systems are used for which large amount of charges are stored in a capacitor bank and discharged them in a short period of time (20 ms∼0.5 s) to a magnet. The highest and meaningful magnetic field for physical experiments for a capacitor-driven pulsed magnet is around 60∼80 T along with ∼25 ms transient time of the field. Such a capacitor-driven pulsed-magnet requires liquid nitrogen to cool the magnet and consumes small electrical power, it is a cost-effective preferable system. However, due to the short transient pulse time, experiments under pulsed-magnetic fields are limited. To enlarge the transient time, a motor-generator type power supply system was introduced for long pulse magnet. Magnetic fields of a generator-driven pulse is typically as high as 60 T and the pulse transient time is around 2 s (see Fig. 1). The virtue of long pulse magnet is not only a long transient pulse time but also reduced eddy current heating. When a metallic sample located in time-varying magnetic fields, eddy current is induced which is proportional to the time derivative of magnetic field (dB/dt). Consequently, fast-varying pulsed magnetic fields generate large eddy current induced heating to any conducting materials which deteriorate low temperature properties of samples. The advent of power generator driven long pulse magnet system made it possible to measure low temperature properties of conducting samples. Recently, a concentric hybrid-type pulsed magnet consisted by an outer generator-driven and an inner capacitor-driven magnets are operated by the National high magnetic Field Laboratory at the Los Alamos Pulsed Field Center which offers up to 100 T. Destructive magnet system which can generate over 100 T to 700 T within few microseconds. We do not discuss any further about destructive type pulsed-magnets.

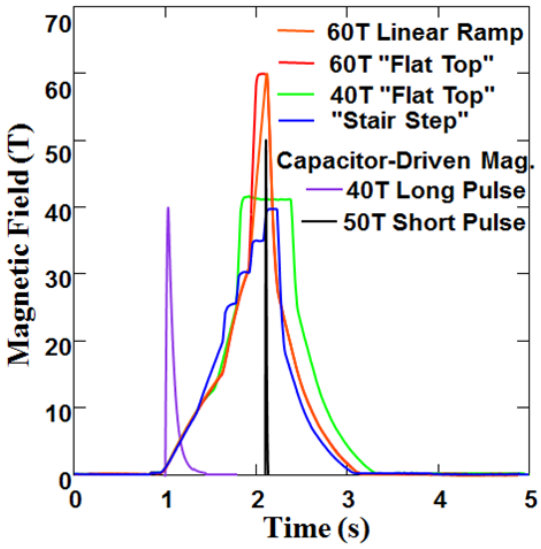

Figure 1. Pulsed magnetic field profiles. Capacitor-driven short pulse magnet has only 25 ms spike-like transient time (black line). Capacitor-driven mid pulse magnet has ∼ 0.5 s field duration (violet) and optical measurements can be made continuously at every 2 ms spectrum acquisition time during the pulse using charge coupled device (CCD) detector. Power generator-driven long pulse magnet has 2 s fields duration with various pulse modes are available.

2. Physical properties of low dimensional semiconductors under magnetic fields

At low temperature, there exist various sources of bound state charges. For example, an ionized donor attracts an electron to consist a hydrogen-like bound exciton. An electron and a hole also construct a hydrogen-like free exciton (X). For a direct band gap intrinsic semiconductor, external excitation such as laser light can excite electrons in the valence band to the conduction band leaving holes behind. Such electron-hole pair forms a free exciton, so called Wannier

exciton. It is expected that ionized hydrogen-like charged exciton structures such as two electrons bound to a hole (X^-) or two holes with an electron (X^+) are able to be formed [4]. In a bulk (3D) semiconductor crystal, due to the small binding energy of charged excitons, it is difficult to detect them. However, in 2D quantum wells, binding energies of charged excitons are detectably enhanced.[5] In the presence of magnetic field, when a charged exciton satisfies the selection rule of $\Delta s=\pm 1$ where s is spin angular momentum of particles, they recombine and generate a photon with right or left circular polarization (RCP, LCP). In a strain-induced semiconductor heterostructure, due to the heavy- and light-hole mixing, linearly polarized photons can be generated.

For a doped semiconductor, due to the screening within the majority carriers, Coulomb attraction between free electrons and free holes are negligible. As a consequence, in a doped semiconductor, formation of exciton is prevented. In this case, a simple free carrier recombination is detected. The main difference between exciton and free carrier recombination is the amount of transition energy. Normally, carrier transition energy (E) between a free electron and a free hole is the same as the band gap (E_g) of the given semiconductor whereas an exciton transition energy differs by the amount of binding energy (E_b) from the band gap, $E=E_g-E_b$. Exciton binding energies in semiconductors vary from ~5 meV (GaAs) to ~60 meV (ZnO) depending on materials. Therefore, GaAs can not form excitons at room temperature whereas excitons in ZnO survive above the room temperature. In the presence of magnetic field, excitons undergo diamagnetic energy shift and free carriers form Landau level transitions. The quantized Landau energy levels are,

$$E_n = \left(n + \tfrac{1}{2}\right)\hbar\frac{eB}{m} = \left(n + \tfrac{1}{2}\right)\hbar\omega_c \qquad (1)$$

where n, e, m, and B are integer numbers, electric charge, electron mass and external magnetic field, respectively, and $\omega_c=eB/m$ is cyclotron frequency. The selection rule for the radiative recombination between the conduction and the valence band Landau levels is $\Delta n=0$ (see Fig. 2). However, the selection rule can often be broken due to the impurities in the quantum system at very low temperature below 4 K. From this equation, we know that the carriers obtain quantized magnetic energy which is proportional to external magnetic fields. However, in specific magnetic fields, due to the strong correlations within 2D free carriers, optical and transport phenomena exhibit integer and fractional quantum Hall effects which means that the Landau energy is no longer linear in B at the quantum Hall states.

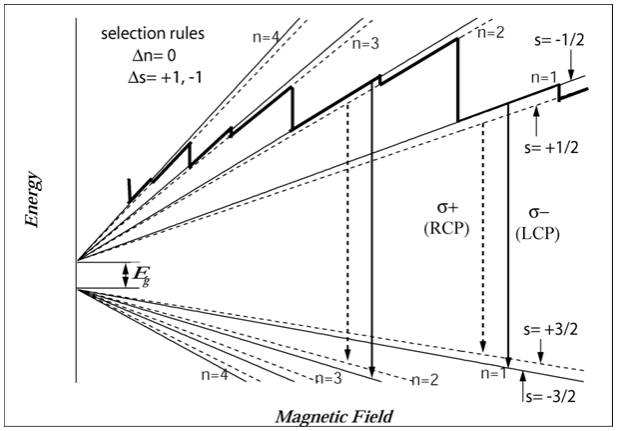

Figure 2. Formation of Landau levels in magnetic fields. Two selection rules for optical transitions are depicted. Selection rule for Landau level transition is $\Delta n=n_{\text{conduction band}}-n_{\text{valence band}}=0$. Each Landau level splits two spin levels which are ±1/2 for conduction electrons and ±3/2 for valence holes. Solid arrow and dashed arrow indicate left circularly polarized (LCP) and right circularly polarized (RCP) photons after recombinations. Thick solid line exhibits the oscillating behavior of the Fermi energy with increasing magnetic fields. When the Fermi energy jump from higher to lower Landau levels, the integer quantum Hall effect occurs.

II. Experimental Setups in Magnetic Fields

Optical fibers are superb experimental tool for spectroscopic measurements in solenoid magnets. For photoluminescence (PL) measurements, single optical fiber can bring external excitation (laser light) to sample and the same fiber carries the signal back to a spectrometer. For magneto-Raman, reflectivity, or absorption measurements, it takes two optical fibers, one for bringing external light source to the sample and the other for carrying signals back to a spectrometer. We have studied magneto-photoluminescence (MPL) properties of semiconductor quantum structures using fiber optic probes to in continuous (to 18 T) and pulsed (to 65 T) magnetic fields applied parallel (Faraday geometry, $B \perp z$) to the growth axis of the 2D layers including modulation-doped and undoped quantum wells, and single interface structures [6]. As seen in Fig. 1, an external excitation from He-Cd, Ti:Sa, or Nd:YAG laser is focused by a small mirror at the one end of an optical fiber which carries the external laser light to the sample at the center of a magnet. The sample is immersed in an L^{4}He flow cryostat (or ^{3}He refrigerator) and a polarizer (circular or linear) is positioned between the sample and the optical fiber. Simply reversing the magnet field, one can change the direction of out coming PL polarization ($\sigma = \vec{B} \cdot \vec{s}$). The same optical fiber carries out coming PL signal and disperse it to the spectrometer. On the right corner of Fig. 3, the Voigt geometry of optical measurement is depicted. In this case, a sample and a linear polarizer is 90° rotated and the magnetic field is along the in-plane direction of quantum structures. A right angle prism is located between the fiber and sample which reflect the external light and PL signal without loss. In this geometry, distinguishing the circularly polarized light does not mean anything because the rotating electric field by circular polarizer interact with external magnet field which breaks the polarization of the light.

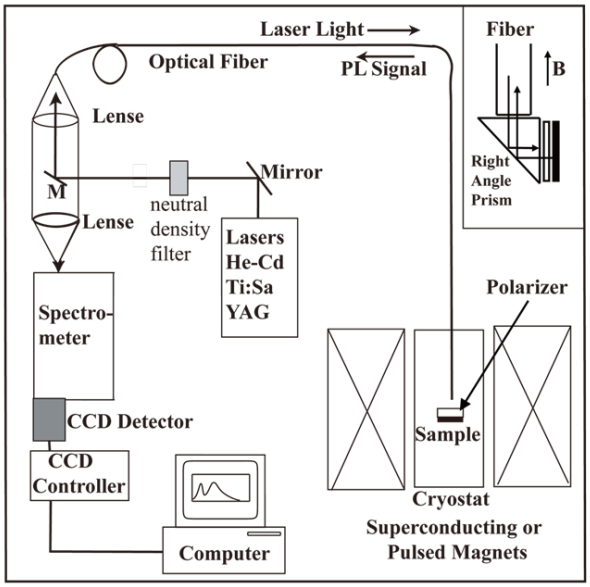

Figure 3. Experimental set up for optical spectroscopic measurements. A multi-mode optical fiber carries laser light to and photoluminescence signal from the sample located at the center of the magnet. Fast CCD detector system made it possible to take a PL spectrum at every 2 ms during transient magnetic field pulse. The inset on the right corner depicts Voigt geometry by using a small right-angle prism.

The spectroscopic measurements have been made at the National High Magnetic Field Laboratory, Los Alamos National Laboratory (NHMFL-LANL), Pulsed Field Facility. Magneto-photoluminescence (MPL) measurements were performed at 4 and 77 K up to 18 T in a superconducting magnet and to 50/65 T in a pulsed magnet and 0.5 K in motor generator driven 60 T long pulse magnet. The pulse profiles for various pulsed-magnets at NHMFLLANL are shown in Fig. 1. For a short pulse magnet, a Pockels cell or a mechanical shutter was set to open for 2 ms corresponding to the flat-top region at the peak of the field. The spectra were recorded during this time interval. The spectral range depended on the grating selected in the spectrograph; data were usually taken with a spectral resolution of ~0.05 meV. The excitation energy was provided by individual lines from

a 10 W Ar^+ laser or an Ar^+-pumped Ti-sapphire laser (tunable from 700~1,050 nm) for visible range, and a He-Cd laser for UV range. Different fiber optic probes (140~600 μm diameter) were available. A multimode optical fiber was used as both an input and an output coupler. The sample holder was attached directly to the end of the fiber bundle for easy selection of fiber diameter, DC or pulsed magnet field, or field direction (perpendicular (Faraday geometry) or parallel (Voigt geometry) to the growth axis of the 2D layers). The holder was positioned at the center of the field and was immersed in the cryogenic fluid or in an exchange gas. The power density on the sample usually did not exceed 2 mW/cm^2. The field values were monitored by a small calibrated pick-up coil imbedded in the plastic sample holder.

At low magnetic fields (15 T) the MPL spectral data for undoped GaAs-AlGaAs single quantum wells (SQWs) show a characteristic diamagnetic shift of magneto-excitons; at low fields below 10 T, the diamagnetic energy shift is proportional to B^2 and at high fields (~35 T), the shift becomes linear in B [7]. In the vicinity of 30 T, all undoped QW samples exhibit anti-crossing of the heavy- and light-hole excitons [8] due to valence band mixing effects [9]. Landau transitions corresponding to band to band recombination are observed in modulation-doped GaAs-AlGaAs quantum well structures. Large non-linear effects are observed in the energy and the intensity versus magnetic field as Landau levels in the conduction band cross the Fermi level [10-12]. In a modulation-doped single heterojunction (SHJ), photo-generated electrons play an important role as they can easily transfer into the triangular shaped well at the interface [13-15]. Peak intensity and its energy position in MPL spectra oscillate at the integer quantum Hall states. This oscillatory MPL behaviors in magnetic fields are confirmed in complementary optical Shubnikov-de Hass measurements. The oscillatory behavior of optical and transport data agree well with self-consistent calculation of the variation in the second subband carrier density [16,17].

III. Excitations in Magnetic Fields; Magneto-exciton, Spin Wave, and Skyrmion

1. Mangto-excitons in Undoped GaAs-AlGaAs quantum wells

Excitons in high magnetic fields undergo diamagnetic energy shift. The magnetically obtained energy competes to the electrically confined energy (binding energy). On the other hand, free carriers in magnetic fields undergo cyclotron motion and its energy is quantized into Landau levels, $E=(n+1/2)$. The exciton binding energy in semiconductor is similar to that of hydrogen, which is called effective Rydberg energy, $Ry^* = 16\pi^2\hbar^3\varepsilon^2\varepsilon_0^2 B / m^{*2}e^3$ where ε and ε_0 are dielectric constants of the given semiconductor and vacuum, respectively. When magnetic field is low (typically below 10 T), the term that contains magnetic field in Schrödinger equation can be treated as a perturbation and the diamagnetic energy shift is proportional to B^2/m^{*3}. However, when magnetic field is high, the magnetic energy can no longer be treated as perturbation and the diamagnetic energy shift is proportional to ω_c.

Fig. 4 exhibits diamagnetic energy shift of excitons in undoped AlGaAs-GaAs single quantum well (SQW) samples in pulsed fields up to 65 T at 77 K [6]. Fig. 1(a) shows full spectra from 0 T to 66.0 T of 12 nm quantum well width. At B=0 T, two prominent peaks were observed at 1.535 eV and 1.545 eV which are identified as the transition between the conduction electron and valence band heavy hole (e1-hh1) and light hole (e1-lh1), respectively. The dotted spectrum at B = 0 T is an expand view for better looking. In low field region (0~10 T), the peaks exhibit typical magneto-exciton behavior with a characteristic diamagnetic energy shift [7] which is quadratic in B. The line width (FWHM) increased with increasing mag-

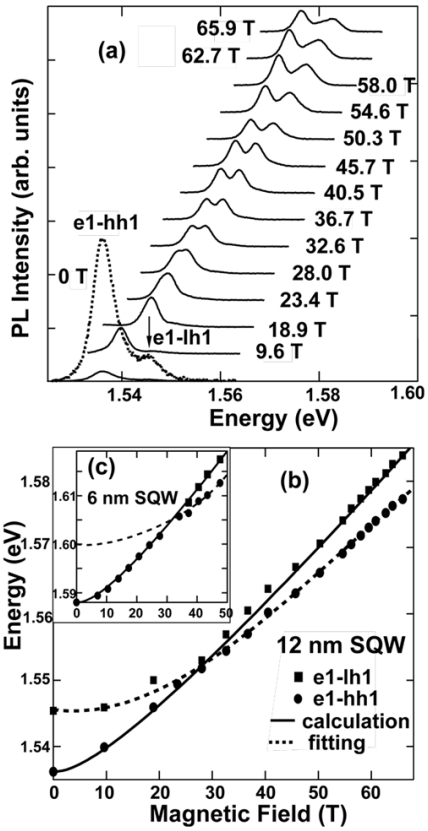

Figure 4. (a) PL spectra in 65 T short pulsed magnetic fields. (b) Energy vs. magnetic field plot. Solid circles and squares below 20 T indicate conduction band to heavy hole transition while solid shows Two peaks clearly show anti crossing behavior.

netic fields. In the high field regime, the shift became linear in B. However, at around 30 T, the e1–hh1 and e1–lh1 transitions intersected and showed anticrossing behavior. Two peaks are getting closer up to around 30 T, and then they move away from each other. The two peaks can be clearly resolved above and below the anti–crossing region. The peak transition energy plotted in Fig. 4(b) clearly shows such anticrossing behavior. Circular and square makers indicate e1–hh1 and e1–lh transitions and solid and broken lines are calculated diamgnatic energy shift without considering valence band maxing. Circular markers initially followed the solid line up to ~30 T and then they followed the broken line whereas the square markers show opposite behavior which

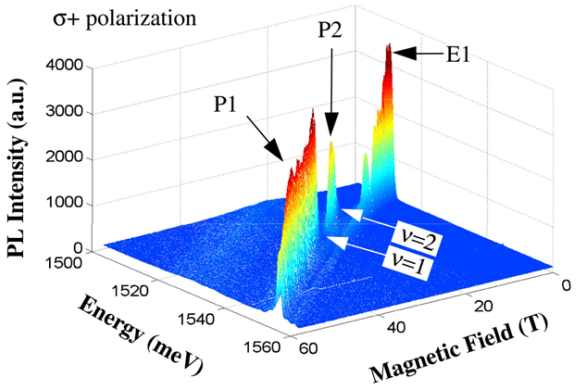

Figure 5. Typical MPL spectra of a GaAs–AlGaAs single heterojunction in long pulse magnet. PL spectra are recorded at every 2 ms interval during the 2 s pulsed magnetic fields.

is a typical anticrossing behavior. With increasing magnetic fields, initially two transitions get close and then push away each other with further increasing magnetic fields. This observation of anticrossing in high magnetic fields is thought to be related to valence band mixing effects of the heavy– and light–hole mixing induced by low–dimensional quantum structure [9]. As seen in the inset of Fig. 4(b), the other sample with 6 nm quantum well width also shows similar anticrossing behavior around 35 T. From the MPL diamagnetic shift data, we estimate the dimensionality parameter, D to be 0.24 for the 6 nm well and 0.47 for the 12 nm well compared with the 3D and 2D limits where exact values for D_{3D}=1 and the D_{2D}=0.19. Our values are about a factor of two less than those reported by Rogers et al. [7] for similar well widths and are closer to the ideal 2D limit.

2. Quantum oscillations in modulation–doped SHJ in magnetic fields

The electric potential profile and the electronic structure of the sample used for this study are depicted in Fig. 5. Due to the band bending which is occurred by modulation doping, the conduction band has wedge–shaped triangular quantum well with quantized

energy levels (E_0 and E_1) whereas the valence band does not have confined energy levels. Consequently, the conduction electrons and the valence holes are spatially separated such a way that photogenerated electrons condensed in the quantum well near the GaAs-AlGaAs interface whereas holes migrate to the GaAs flat band region. We have performed magneto-transport measurement with and without laser illumination to a modulation doped single heterojunction in order to determine the density of two-dimensional electron gas (2DEG) in the quantum well. In the presence of magnetic field, free carriers undergo Landau level splitting. Each Landau level splits into two spin states. Due to negative g-factor of GaAs, spin-up energy level is lower than spin-down level. The Landau level splitting modified the carrier density. It is well known that the density of states in 2DEG is constant. However, due to the Landau level splitting, the density of states are given by delta-function at each Landau levels at 0 K. Because of finite temperature and impurity effects, the density of states show Gaussian broadening. When number of ν Landau levels are filled, the Landau filling factor is defined as,

$$\nu = N\frac{h}{eB} \tag{2}$$

where is N density of 2DEG and h is Plank constant. In Eq. 2, measuring magnetic field for any integer ν, the total 2DEG density (N) can be calculated as

$$N = \frac{e}{h}B_\nu \times \nu = \frac{B_\nu \times \nu}{4.14T} \times 10^{11} cm^{-2} \tag{3}$$

From Eq. (2), the degeneracy of Landau level is than calculated as,

$$\frac{N}{\nu} = \frac{eB}{h} \tag{4}$$

This means that the degeneracy of Landau levels in creases with increasing magnetic field. Consequently, electrons in upper Landau levels move down to lower Landau levels with increasing magnetic field, which leads to gradually empty the upper Landau levels. As upper Landau levels emptied, the Fermi energy jumps from emptied upper level to next lower filled levels. This process repeats with further increasing magnetic field and consequently, the Fermi energy oscillates with increasing magnetic field. Many physical quantities such as magneto-resistance (Shubnikov-de Haas oscillation), heat capacity and magnetization oscillate with the same period of the Fermi energy oscillation.

We made magneto-photoluminescence (MPL) measurements of a series of SHJ samples Table 1 lists the various parameters for the five samples investigated. All the samples had high mobilities: MPL measurements using perpendicular magnetic fields ($B//z$) were performed at 2.1 K from 0 to 18 T in a superconducting magnet and at temperatures of 0.4 and 1.5 K in a 60-T generator-driven long pulse magnet. Right-(σ^+) and left-(σ^-) circularly polarized PL spectra were recorded every 0.2 T from 0 to 18 T; approximately 500 spectra/sec were recorded as the field pulse swept from 0 to 60 in ~2 seconds. The laser excitation wavelength was either 633 nm (HeNe) or 635 nm (diode laser) and did not exceed 0.2 mW/cm^2 in the superconducting magnet and 1.5 mW/cm^2 in the long pulse magnet. The measured 2D carrier densities (see Table 1) ranged from 1.2 to 7.2×10^{11} cm^{22}.

Fig. 5 displays typical PL spectra of the SHJ sample taken at 4 K as a function of magnetic field for $B//z$ using generator-driven long pulse magnet. At B=0, the spectrum consists of three peaks located at 1515.5, 1514.0, and 1510.5 meV. The middle peak is the most intense and is related to the radiative excitonic recombination of the $E1$ subband with photo-created holes close to the top of the valence band in

Table 1. Sample parameters and the calculated electron–hole separations. $d_{e-h}(1)$ includes corrections to B_{SW} only; $d_{e-h}(2)$ includes corrections to both B_{SW} and B_X.

Sample no.	n2D (10^{11}/cm^2)	Mobility (10^6 cm^2/V · s)	ΔE_1 (meV)	$d_{e-h}(1)$ (Å)	$d_{e-h}(2)$ (Å)
10.19.89.1.0	1.84	7.7	0.8	105	40.5
10.24.89.1.2	2.06	7.4	1.4	110	42.5
09.18.91.2	2.5	3.4	0.9	70	30
EMC 716	5.9	1.5	2.5	30	16.5
EMC 712	7.2	1.2	2.5	25	14
G640 (Ref. 9)	1.17	not avail.	1.0	230	77
G650 (Ref. 9)	2.26	not avail.	2.0	100	45
G627 (Ref. 9)	3.2	not avail.	2.6	70	34

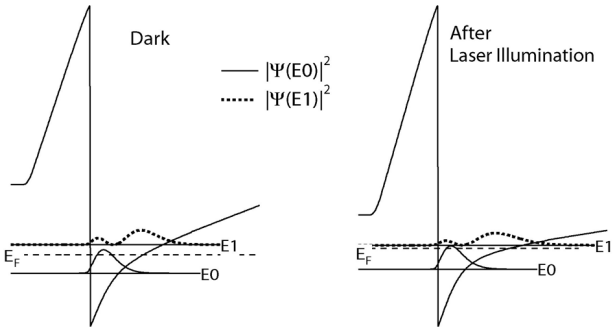

Figure 6. Calculated energy levels and wavefunctions. After laser illumination, as the potential well changed, the energy levels (E_0, E_1) and Fermi energy increased.

the GaAs layer. The higher-energy peak of medium intensity at 1514.0 meV is possibly due to the free exciton (FX) in bulk GaAs. The low-energy peak of weak intensity probably emanates from excitons bound to an ionized acceptor (A^-–X). The intensity of the FX peak and the A^-–X peak decrease with increasing magnetic field, and show a diamagnetic shift characteristic of excitonic transitions in the low field regime. Energy scans were taken at 0.2 ms intervals to 60 T. Intensity oscillations and small energy deviations (steps) from linear behavior for the E_1 exciton transitions were observed over this magnetic-field range.

Before illuminating the sample with laser light, the electron density in the well is about 4.58×10^{11} cm^{-2}, and our theoretical calculation shows that the E_0 and E_1 energy levels and the Fermi energy lie at 47.7, 73.1, and 64.2 meV from the bottom of the well, respectively. The energy separation between the Fermi energy and the E_1 subband is about 8.9 meV. After illuminating the sample, the electron density in the well increased to 5.82×10^{11} cm^{-2}, and the $E0$ and E_1 energy levels change to 51.2 and 72.8 meV from the bottom of the well, respectively (see Fig. 6). Another interesting result of our calculation is that the Fermi energy is located at 0.67 meV below the empty E_1 subband. Due to this close proximity of $E1$ and the Fermi energy, strong Coulomb interaction between 2DEG and the excitons influence the magnetoexciton emission [8]. The intensity modulation has the same period as the Shubnikov-de Haas oscillation; this is in good agreement with Ref. 8.

In Fig. 7, intensity minima occur when the Fermi energy is located in the extended states, whereas the energy maxima occur when the Fermi energy is located in the localized states. A Coulomb interaction between the 2D electron gas and the exciton state leads to the intensity modulation. When a Landau level of the 2D electron gas in the E_0 subband crosses the E_1 exciton state, due to a Coulomb interaction, corresponding eigenstates are hybridized. This enhances the interband matrix element for the overlapping transitions. When the Fermi energy crosses the E_0 Landau levels, it changes the electron density

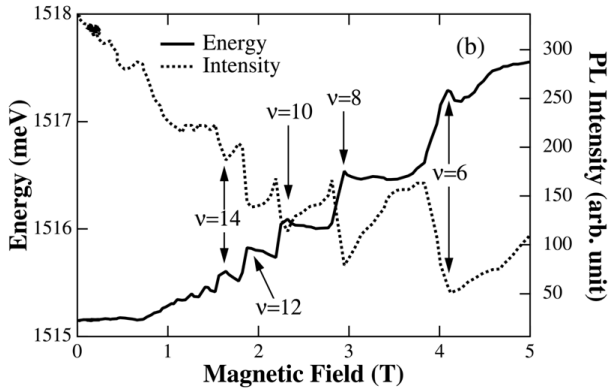

Figure 7. Intensity and transition energy oscillations in magnetic fields. At the integer quantum Hall regions, intensity minima occur which coincide with energy maxima. These quantum oscillations are due to the strong correlation within free carriers.

in the E_0 Landau levels that modulate Coulomb interactions between a 2D electron gas and an E_1 exciton. This periodic change of the Coulomb interaction modulates the MPL intensity [8].

The nonlinear behavior of the transition energy is more complicated. When the Fermi level sweeps through an extended state, the screening strength changes, because screening within 2DEG is proportional to density of states at the Fermi level. Repeating this process with changing magnetic fields modulates the screening strength, which leads to a nonlinear behavior of the transition energy in an optical process. Hawrylak, Polsford, and Ploog [13] reported that energy oscillations can be eliminated by acceptor doping in a single heterojunction, while the PL intensity continues to oscillate with varying magnetic fields. With acceptor doping, hole screening is negligible because holes in the valence band are blocked by the doped acceptors, and electrons can "see" only the acceptors. A theoretical study [9] also has shown that energy variation occurs at the even numbers of integer quantum Hall states due to the screened exchange and Coulomb hole self-energy. However, it is suggested that the Coulomb hole of the hole term is dominant, since the electron exchange and correlation are effectively canceled, and insufficient photo-created holes exist to make the hole correlations while suppressing the exchange energy [18].

3. Spin wave and skyrmion states at ν=1 quantum hall state

At ν=1, all conduction electrons stay in the lowest Landau level spin up state and therefore, it forms a quantum ferromagnetic state. At such state, the Fermi level is located at the localized state and the density of state at the Fermi level is ideally zero. This means that at ν=1 quantum Hall state, screening within the 2DEG is completely negligible. Consequently, new low lying excitations appear such as charged excitons, spin waves or Skyrmions. In a doped quantum well, due to the screening within 2DEG, the formation of excitons is prohibited and the optical recombination occurs between free electrons and holes. However, without screening, an electron in the conduction band and a hole in the valence band can form a bound state called exciton (X) analogous to hydrogen atom (H). For a doped quantum well, due to excess carriers in the conduction band, two electrons can compose a bound state with single hole which is called negatively charged exciton (X^-) similar to negatively charged hydrogen atom (H^-).

Spin wave is an exciton complex within the conduction band. As seen in Fig. 8(a), at ν=1, initially, all the conduction electrons stay in the LLL spin up state. When an electron is excited from the valence band, than this electron naturally stays in the LLL spin down state in the conduction band because the spin up state is fully occupied and therefore there is no available state at the LLL spin up level. If the electron in the LLL spin-down state recombines with the valence hole, the final state becomes the same as the initial state, which is the exciton recombination at the ν=1. However, if an electron in the LLL spin-up state recombination with the valence hole, it

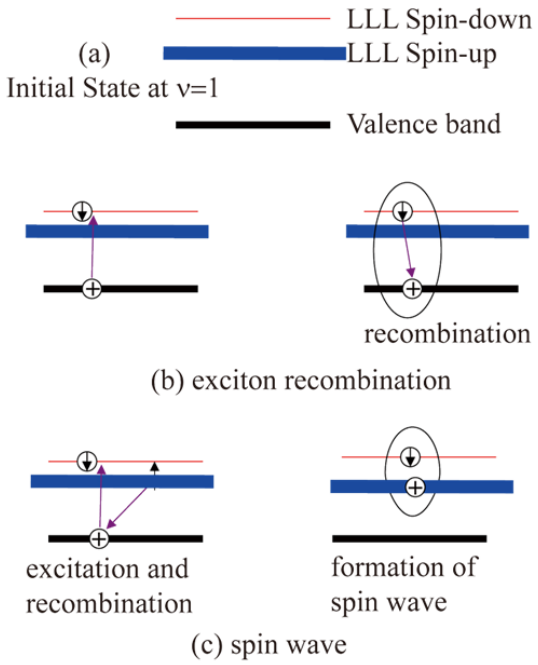

Figure 8. Schematic diagram of the formation of exciton and spin wave. (a) At ν=1, LLL spin up state is completely filled and the LLL spin-down is completely emptied. (b) An excited electron from the valence band jump to the LLL spin-down level (left) and then it recombines to the valence hole. Therefore, for the exciton recombination, the initial and the final state are the same. (c) If an electron in the LLL spin-up state recombines to the hole (left), the final state becomes a spin- down electron and a spin-up virtual hole in the LLL spin-up level consist a spin wave.

leaves a virtual hole in the LLL spin-up state. In this case, the final state becomes a bound state of spin-down virtual hole with the electron in the LLL spin up state, therefore, the formation of the spin wave takes place.

Skyrmion is another low lying excitation at the $\nu=1$ quantum Hall state. When the very last electron in the LLL spin-down state in the conduction band moves down to the LLL spin-up state at the $\nu=1$, that electron has to rotate its down-spin to up-spin. However, instead of rotating its down-spin, it twist other up-spin electrons which globally rotates all electron spins in the LLL spin-up level. Such twisted

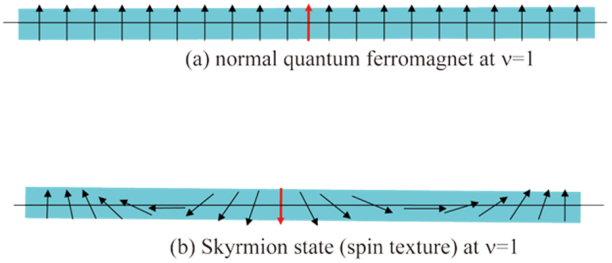

Figure 9. (a) When a spin-down electron comes into the spin-up level and turns its spin orientation up, it becomes normal quantum ferromagnetic state at ν=1. (b) When a spin-down electron comes into the spin-up level and twists other spins, formation of the Skyrmion state takes place.

spin texture is called Syrmion as seen in Fig. 9(b). Skyrmion is a soliton with the total spin of zero. It is known that the strong Coulomb interaction between the conduction electron and the valence hole prevent from forming Skyrmions. Therefore, it requires spatial separation between electrons and holes to reduce Coulomb interaction for the formation of the Skyrmion.

In Table 1, the measured redshifts in energy (ΔE_1), at filling factors $\nu=1$ were obtained from plots similar to those shown in Figs. 10(a) and (b). The related sample parameters (carrier concentrations and mobilities) for all the SHJ's investigated are also listed in Table 1. The corresponding redshifts for three samples reported by Nicholas et al.[19] were estimated from Fig. 1 in their paper and are also shown in Table 1 together with other sample parameters where known. The distance between the electron and the hole layers d_{e-h} was calculated using Eqs. (22)~(25) outlined in the paper by Cooper and Chklovskii [19]. The redshifted energy ΔE_1 at $\nu=1$ is related by

$$\Delta E_1 = B_{SW} - B_X, \tag{5}$$

where B_X is the binding energy of the exciton formed in the initial state. B_{SW} is the binding energy of the spin wave formed in the +1/2 electron level and

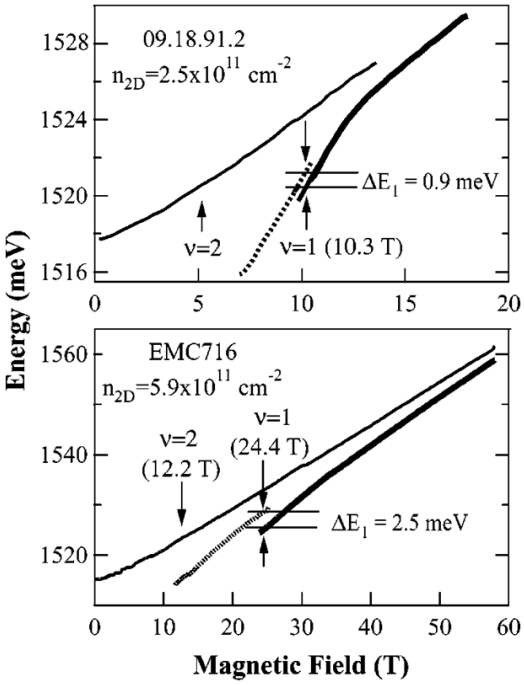

Figure 10. Plot of the observed MPL transition energies, FX (thin solid line), X (dotted line), and e-FH (thick solid line) for two representative samples: (a) n_{2D}=2.5×10^{11} cm^2 and (b) n_{2D}=5.9×10^{11} cm^2.

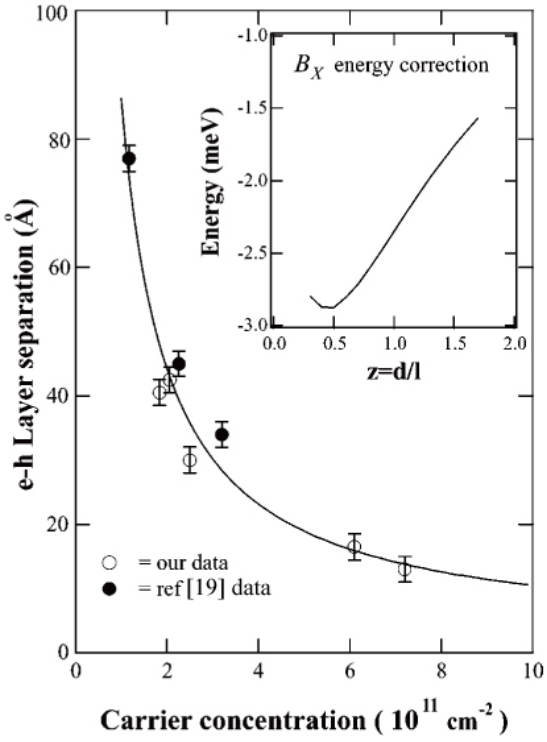

Figure 11. Plot of the calculated electron-hole separation, $d_{e-h}(2)$ from Table 1 as a function of carrier concentration. The solid line is a simple fit to the data with an inverse dependence of d_{e-h} with carrier concentration. The second-order correction to the excitonic binding energy B_X as a function of d/l is shown in the inset.

was calculated by Cooper and Chklovskii [20] as the excitonic binding energy when the separation between particles reduces to zero. For any nonzero d_{e-h}, B_X is less than B_{SW} and the free hole state will always be the lower energy state. As the magnetic field is swept from $\nu > 1$ through $\nu < 1$, one may expect to see a transition from an excitonic (X^0) state to a free hole state (e-FH) with a resulting redshift in the PL energy. The binding energy of the excitons B_X is given by

$$B_X = \sqrt{\frac{\pi}{2}} e^{d^2/2l^2} erf(d/\sqrt{2}l) \frac{e^2}{4\pi\varepsilon\varepsilon_0 l}, \quad (6)$$

and the binding energy of the spin wave (or Hartree-Fock energy) B_{SW} as

$$B_{SW} = \sqrt{\frac{\pi}{2}} \frac{e^2}{4\pi\varepsilon\varepsilon_0 l}, \quad (7)$$

where l is the cyclotron radius.

Cooper and Chklovskii [20] included the effects of Landau level mixing of the electrons in their calculations by considering changes in B_{SW} and B_X to second order in the Coulomb interaction. The B_{SW} value obtained from Eq. (7) should be modified using Eq. (24) in their paper. This second-order correction to B_{SW} was calculated by Sondi et al. [27] and they found that B_{SW} decreased by 6.77 meV for a GaAs system, a result which is independent of magnetic field and "d." In our evaluation of Eq. (24) [20], we used a value of ε=12.8 and obtained 6.13 meV for this correction. The second-order correction to the excitonic binding energy B_X was derived in Appendix C and is summarized in Eq. (25) of Ref. 19. They showed that the correc-

tion to the binding energy of the exciton is less than correction to the binding energy of the spin wave. However, the B_X correction depends on the d/l ratio as seen in the inset in Fig. 11. Inclusion of this correction to B_X in our samples significantly reduces the calculated d_{e-h} distances as seen in Table 1. Here we present the calculated distances between the electrons and holes near the interface for our SHJ samples and for those measured by Nicholas et al. [19] The last two columns in the table show the calculated layer separations as a function of the carrier concentration for the BSW energy correction only [$d_{e-h}(1)$] and with both the B_{SW} and B_X corrections [$d_{e-h}(2)$]. The error in ΔE_1 is estimated to be ± 0.07 meV. The error in $d_{e-h}(2)$ with both corrections included is estimated to be about 62 Å. We find that the separation decreases with increasing carrier concentration as may be expected and it can be described approximately by an inverse dependence as shown by the solid line in Fig. 11. This dependence results from the Coulomb interaction between the 2DEG at the interface and the nonlocalized holes. The holes will tend to locate in a position in the valence band that minimizes the potential energy. We appreciate that this picture is rather approximate as it in no way takes into account the finite thickness of the hole layer. Nevertheless, in SHJ samples with moderate to high carrier concentrations, it explains why the recombination intensity for $2>\nu>1$ and $1>\nu>1/3$ in particular is so strong. The wave function overlap between the 2D electrons in the CB and the free holes in the valence band could be comparable or larger than those designed in SHJ's that were specifically doped with Be acceptors (typically about 20～25 nm from the interface) [22,23]. Our analysis shows that the free holes even in lightly doped materials (e.g., $\sim 1.2\times 10^{11}$ cm^{-2}) may be located much closer to the interface than SHJ's studied using delta-doped acceptor bound holes.

For large values of d_{e-h}, the spin wave state will no longer be the ground state. Its place will be taken by a state where the valence hole binds to an electronic spin texture, in which more than one electron presents some degree of spin depolarization leading to the formation of an excitonic Skyrmion. However, in our samples, the calculated d_{e-h} are too small to form the Skyrmion state. The lowest d_{e-h} extracted in Ref. 18 is about 80 Å as seen in Fig. 11 which is in the regime of the formation of Skyrmion state.

IV. Summary

Photoluminescence measurements in pulsed magnetic fields to 65 T at low temperatures were established at NHMFL-LANL. We have undertaken a comprehensive investigation of magnetoexcitonic and Landau transitions in a large variety of undoped and modulation doped (2DEGs) QW heterostructures. A He3 exchange gas cryostat allows optical studies to be made below 0.5 K in fields as high as 60 T. From undoped SQWs, we realized that heavy and light hole anticross in high magnetic fields around 30 T. For doped SHJs, strong correlation effects such as PL intensity and energy oscillations, and discontinuous transitions at integer quantum Hall regimes were observed in the presence of strong magnetic field. For the future works, one-dimensional quantum wire or nano-belt type low dimensional semiconductor heterostructures will be preferable, because reduced dimensionality might generate new correlations within free carriers. In addition, a capacitor-driven 50 T mid-pulse (～0.5 s) magnet system is under construction in the department of Applied Physics at Dankook University. The capacitor bank is consisted by 50 capacitors with total stored energy of 1.6 MJ. It will offer various physical measurements in ultra high magnetic fields such as optical spectroscopy, de Haas-van Alphen effect and magneto-transport.

Acknowledgement

This research was supported by Leading Foreign Research Institute Recruitment Program through the National Research Foundation of Korea (NRF) funded by the Ministry of Education, Science and Technology (MEST) (No.2013-044975).

References

[1] K. von klitzing, G. Dorda, and M. Pepper, Phys. Rev. Lett. **45,** 494 (1980).

[2] D. C. Tsui, H. L. Störmer, and A. C. Gossard, Phys. Rev. Lett. **48,** 1559 (1982).

[3] D. Heiman, in: D. G. Seiler and C. L. Little (Eds.), Semiconductors and Semimetals, Vol. 36, Ch. 1, Academic press New York, 1992, p. 1 and references therein.

[4] M. A. Lampart, Phys. Rev. Lett. **1,** 450 (1958).

[5] B. Stébé and A. Ainane, Superlattices Microstruct. **5,** 545 (1989).

[6] C. H. Perry, Y. Kim, and D. G. Rickel, in: Z. Fisk, L. Gorkov, D. Meltzer, and R. Schrieffer (Eds.), Physical Phenomena at High Magnetic Fields II, World Scientific, Singapore, 1995, pp. 97-102.

[7] D. C. Rogers, R. J. Nicholas, C. T. Foxon, and K. Woodbridge, Phys. Rev. B **34,** 4002 (1986).

[8] Y. Kim, C. H. Perry, K-S. Lee, and D. G. Rickel, Bull Am. Phys. Soc. **42,** 373 (1997).

[9] E. Y. C. Yang and L. Sham, Phys. Rev. Lett. **58,** 2598 (1987).

[10] C. H. Perry, J. M. Worlock, M. C. Smith, and A. Petrou, in: G. Landwehr (Ed.), High Magnetic Fields in Semiconductor Physics, Springer Series in Solid State Sciences, vol. 71, Springer, Heidelberg, 1987, p. 202.

[11] B. B. Goldberg, D. Heiman, A. Pinczuk, L. Pfei¤er, and K. West, Phys. Rev. Lett. **65,** 641 (1990).

[12] M. Dahl, D. Heiman, A. Pinczuk, B. B. Goldberg, L. Pfeiffer, and K. West, Phys. Rev. B **45,** 6957 (1992).

[13] P. Hawrylak, N. Pulsford, and K. Ploog, Phys. Rev. B **46,** 15193 (1992).

[14] K. S. Lee and E. H. Lee, J. Appl. Phys. **76,** 5778 (1994).

[15] K. S. Lee and E. H. Lee, Phys. Rev. B **51,** 13315 (1995).

[16] Y. Kim, C. H. Perry, D. G. Rickel, and K-S. Lee, Bull. Am. Phys. Soc. **41,** 240 (1996).

[17] K-S. Kee, E. H. Lee, C. H. Perry, and Y. Kim, Inst. Phys. Conf. Ser. **145,** 459 (1996).

[18] Y. Kim, F. M. Munteanu, C. H. Perry, D. G. Rickel, J. A. Simmons, L. N. Pfeiffer, and K. W. West, Phys. Rev B **64,** 195302 (2001)

[19] R. J. Nicholas, D. Kinder, A. N. Priest, C. C. Chang, H. H. Cheng, J. J. Harris, and C. T. Foxon, Physica B **249,** 553 (1998).

[20] N. R. Cooper and D. B. Chklovskii, Phys. Rev. B **55,** 2436 (1997).

[21] S. L. Sondhi, A. Karlhede, S. A. Kivelson, and E. H. Rezayi, Phys. Rev. B **47,** 16 419 (1993)

[22] I. V. Kukushkin, N. Pulsford, K. von Klitzing, K. Ploog, and V. B. Timofeev, Surf. Sci. **263,** 30 (1992).

[23] M. Hayne, A. Usher, A. S. Plaut, and K. Ploog, Phys. Rev. B **50,** 17208 (1994).